Carbon isotopes show snowpack acts as a valuable moisture subsidy to mountain forests in the Oregon Cascades

By

Christopher J. Ratcliff

An Undergraduate Thesis Submitted to

Oregon State University

In partial fulfillment of
the requirements for the
degree of

Baccalaureate of Science in BioResource Research,
Water Resources Option,
Biosystems and Climate Modeling Option

June 10th, 2015

CARBON ISOTOPES SHOW SNOWPACK ACTS AS A VALUABLE MOISTURE SUBSIDY TO MOUNTAIN FORESTS IN THE OREGON CASCADES

CHRISTOPHER J. RATCLIFF [1], STEVEN L. VOELKER [2], ANNE W. NOLIN [3]

1. Department of BioResource Research, Oregon State University, Corvallis, OR 97330 USA
2. Department of Forest Ecosystems & Society, Oregon State University, Corvallis, OR 97330 USA
3. College of Earth, Ocean, and Atmospheric Sciences, Oregon State University, Corvallis, OR 97330 USA

Keywords: isotopes, drought, latewood, mountain forest, snowpack, climate change, water, watershed.

Primary Research Paper

Abstract

This study examines climatological influences, particularly that of snowpack, on tree growth and stable carbon isotope discrimination ($\Delta^{13}C$) from ~1980 to 2013 at two sites located in the upper reaches of the McKenzie River watershed of the Oregon Cascade Mountains. We tested the use of $\Delta^{13}C$ values from latewood, corroborated by tree-ring width chronologies as precipitation proxies to develop correlations between moisture stress and climate variables. Tree species at each site included Douglas-fir and mountain hemlock. Interpolated meteorological and snowpack data included snow water equivalent (SWE), precipitation, atmospheric temperature, vapor pressure deficit (VPD), relative humidity (RH), and a metric estimating growing season length. Significant correlations between latewood $\Delta^{13}C$ and winter SWE at each site indicated the importance of winter snowpack to our selected tree species (r = 0.35, r = 0.43). Late summer precipitation and relative humidity (RH) were also significantly correlated with $\Delta^{13}C$ (r = 0.49, r = 0.46; r = 0.43, r = 0.44). High correlations at both sites reinforced that late summer VPD was the primary driver of $\Delta^{13}C$ (r = - 0.67, r = -0.61), which is often associated with moisture stress. This was further supported by correlations between air temperature and $\Delta^{13}C$ (r = -0.46, r = -0.47), which drives much of the variation in VPD. Growing season length also showed significance in mountain hemlocks at the site with longer average snowpack (r = -0.22, r = -0.44). Moisture supplied by spring snow melt is a seasonably limited resource, nonetheless both sites clearly showed that snowpack acts as a valuable moisture subsidy to coniferous mountain forests in the Oregon Cascades. This study acts as a useful case study for future investigations into the relationship between snowpack and forest health in the Pacific North West.

Introduction

Mountain forests are crucial regulators of river and stream water discharge and carbon cycling in many regions of the world. However, wildfires, pest outbreaks, and droughts are threats to mountain forests that are intensifying as a consequence of global climate change (Van Mantgem et al., 2009; Williams et al., 2013; Westerling et al., 2006). Contemporary climate models show that by midcentury the mean forest-moisture stress in the southwest United States (SWUS) will surpass that of the most severe droughts in the past millennium (Williams et al., 2013). The present drought in the SWUS since the turn of the century is the fifth strongest noted drought since 1000 AD (Williams et al., 2013). Similar drought patterns have been observed over the last 6,000 years in the Pacific Northwest, via moisture-sensitive tree-ring records and lake sediment cores (Nelson et al. 2011). The current drought in California is encroaching into the Pacific North West potentially decreasing available precipitation and increasing water stress deficits. Current droughts pose a significant threat to forest functionality; increasing the probability of forest fires, pest outbreaks, and attack by tree-killing pathogens (Van Mantgem et al., 2009; Williams et al., 2013).

Recent examination of the relationship between montane forests and hydrology has established that inter-annual variations in snowpack accumulation are positively correlated with forest productivity (Trujillo et al., 2012; Roden & Ehleringer, 2007). Shifts toward earlier snowmelt have also been shown to increase forest fire activity and mortality of mountain forests (Westerling et al., 2006; Trujillo et al., 2012; Peterson & Peterson, 2001). For a 2°C increase in winter temperature, peak snow water equivalent (SWE), the water content of snowpack, in the western Oregon Cascades is predicted to decrease by 62%, while shifting the date of peak SWE 22 days earlier (Sproles et al., 2013; Eq. 3). Fluctuations in snowpack associated with climate change may have a detrimental effect on mid-elevation forests of the Cascades, environments which provide a wealth of ecosystem services including biomass based energy, renewable resources, climate regulation, nutrient cycling, and water control and supply. Despite research

investigating the response of native forests to drought and climate factors, connections between decreasing snowpack and forest productivity in the Oregon Cascades are still poorly understood.

Stable carbon isotope discrimination and tree-ring width chronologies have been used as proxies for tree moisture stress in previous studies in the western United States (Roden & Ehleringer, 2007; Leavitt et al., 2010). Summer precipitation was shown to influence stable carbon composition of ponderosa pine tree-ring cellulose through the effects of plant water status (Roden & Ehleringer, 2007). The foundation of this relationship is largely driven by stomatal closure, which constrains gas exchange between the tree and atmosphere when trees incur drought stress (McCarrol & Loader, 2003). When stomata close due to water stress they reduce intercellular CO_2 concentrations, which in turn reduces discrimination against $^{13}CO_2$ over $^{12}CO_2$ by Rubisco, a photosynthetic enzyme that carboxylates carbon dioxide (Farquhar et al., 1982). In this way $\delta^{13}C$ and $\Delta^{13}C$ signals can act as precipitation proxies that will decrease or increase according to the relative water stress of the tree. Stable isotope ($\delta^{13}C$) signals are expressed in permil notation (Craig, 1957), where the 13C/12C ratio (R_{sample}) is held relative to a standard (PeeDee Belemnite) that has an anomalously high $^{13}C/^{12}C$ ($R_{standard}$) ratio as follows:

$$\delta^{13}C = \frac{R_{sample} - R_{standard}}{R_{standard}} \; x\ 1000 = ‰ \qquad \text{(Eq. 1)}$$

Using this notation, most natural materials have a negative $\delta^{13}C$ value. The resulting $\delta^{13}C$ values are then used to calculate isotope discrimination ($\Delta^{13}C$) as follows:

$$\Delta^{13}C = (\delta^{13}C_a - \delta^{13}C_p) / (1 + \delta^{13}C_p / 1000) \qquad \text{(Eq. 2)}$$

where $\delta^{13}C_a$ is the average carbon isotope signal of the ambient atmosphere for a given year and $\delta^{13}C_p$ is that of plant tissue. Variation in $\Delta^{13}C$ accounts for the long-term trend of decreasing $\delta^{13}C$ since the early 19th century caused by fossil fuel emissions that have decreased atmospheric $^{13}CO_2$ (Keeling et al., 2001; Eq. 2). Conversion to $\Delta^{13}C$ causes the correlations with climate variables to have an opposite sign compared to $\delta^{13}C$. For example, positive correlations between $\delta^{13}C$ and a climate element implies it is driving moisture stress, but positive correlations with $\Delta^{13}C$ implies that element is acting as a moisture subsidy and inhibiting moisture stress. Latewood cellulose $\delta^{13}C$ values have been negatively correlated with maximum winter snowpack measurements taken from snow telemetry (SNOTEL) stations, implying that in years with higher snowpack trees experience less moisture stress (Roden & Ehleringer, 2007).

Latewood (LW) is one of two types of distinct growth produced in tree-rings of many species. It is formed late in the growing season, when growth rate declines and soil moisture is generally less abundant. LW cells are smaller and have thicker cell walls than cells produced earlier in the growing season. Earlywood (EW) or early season growth is produced during the spring and accounts for 40-80% of a rings growth in most conifers (Domec & Gartner, 2002). EW cells are larger and have thinner cell walls than LW. Within a tree ring, the transition from EW to LW can be abrupt or gradual, depending on the species. In either case, the bright hues of EW provide a distinct contrast with the LW of the preceding year, leading to the perception of concentric rings when a transverse section of a tree stem is viewed. EW cells that developed under low water-stress conditions can better maintain higher turgor pressure (water pressure exerted on cell walls from within) and therefore develop larger lumens and thinner cells walls. LW cells often experience lower turgor pressure due to drier conditions, which can contribute to cells being smaller and having thicker cell walls. These mechanisms result in the distinct differences between LW and EW. In summer-dry ecosystems, the late summer often corresponds to the greatest moisture deficits, impacting LW cell numbers and dimensions. This allows tree-ring width measurements, particularly LW parameters,

to act as precipitation proxies, which in turn can support whether moisture stress, as indicated by variation in LW $\Delta^{13}C$, has a significant effect on tree growth.

To our knowledge no study has directly quantified the relationship between SWE and LW isotopic composition or tree-ring widths in the Oregon Cascades. The overarching goal of this study was to characterize the relationship between SWE and LW $\Delta\ ^{13}C$ as an indicator of late summer moisture stress in mountain forests of the Oregon Cascades. We hypothesized that SWE of the preceding winter would be negatively correlated with late summer moisture stress of coniferous trees.

Study Site

The study area is located in the Oregon Cascades, situated in the headwaters of the McKenzie River Basin (MRB), a 90-mile tributary of the Willamette River and a primary watershed of the Willamette Valley (Figure. 1). Average annual precipitation in the MRB varies greatly by elevation and ranges from 1,000 mm to 3,200 mm (Jefferson et al., 2008). Winter air temperatures remain close to 0°C, so the phase of precipitation is very sensitive to temperature readily shifting from rain, to snow, to a mixture of both (Sproles et al., 2013). The rain-snow transition zone is between 400 m to 1200 m (Tague and Grant, 2004). Above 1200 m, most of the cold season precipitation falls as snow. Snowpack exceeding 2 m of SWE can accumulate providing substantial summertime flow to the basin. The highly porous and permeable basalt geology of the area acts as an aquifer helping maintain stream flow (Lux, 1981). This snowpack is a key resource for the surrounding ecosystem, as well as agricultural and municipal interest. Present day recording of the snowpack is carried out by point-based data via Natural Resource Conservation Service (NRCS) Snowpack Telemetry (SNOTEL) (USDA, Natural Resource Conservation Service, http://www-.wcc.nrcs.usda.gov/snow). The length of the Cascade Crest includes native tree species such as western hemlock, Douglas-fir, and lodgepole pine. This area acts as a prime location to investigate the

relationship between snowpack and LW $\Delta^{13}C$ and growth in coniferous mountain forests of the Oregon Cascades. We selected two mid-elevation SNOTEL sites (Santiam Junction and McKenzie) from which to collect data (Figure 1). Important characteristics of each site are listed in Table 1.

Materials and Methods

Sampling Strategy for Tree Core Selection

Tree core samples were collected in forest areas within 0.25 km of each SNOTEL site (Santiam Junction and McKenzie). Collection sites were located on low ridges about 30 m higher in elevation than the SNOTEL sites in order to minimize any effects due to downslope water drainage that would have reduced water stress. At each site, we ascertained the dominant tree species and selected dominant or codominant individuals to sample. At the Santiam Junction site, we noted that there was an old dirt road leading up to the ridge area so we selected individual trees that were at least 10 m from this road. Tree age, width, and crown growth were all considered when choosing trees to sample. Sampled trees were between 100 and 150 years old to avoid the 'juvenile effect' (Leavitt, 2010). The 'juvenile effect' describes the tendency of tree rings near the pith of the tree, representing earlier years of growth, to have increased $\delta^{13}C$ values possibly due to soil respiration, reduced light, and proximity to the tree crown. At McKenzie (1454 m) mountain hemlock were sampled and at Santiam Junction (1139 m) Douglas-fir were sampled. A circular fixed plot (r = 13.8 m) was set to characterize the tree density and basal area of each stand sampled (Table 1). Tree diameter at breast height (DBH, or 1.6 m) was measured with a steel tape for each tree > 17.8 cm DBH. The coring strategy was guided by information on carbon isotope variability gleaned from the literature. Previous research indicates that inter-tree variability of stable carbon isotope composition

Table 1. Site Descriptions. Mean precipitation and peak SWE values for Santiam Junction and McKenzie were acquired from SNOTEL climate records. Tree stand data was collected within 0.25 km of each SNOTEL site. Abbreviations: BA, basal area; MAP, mean annual precipitation; MPS, mean annual peak SWE.

Site	Location	Elevation (m)	SNOTEL Record (years)	Dominant Species	BA (m^2/ha)	Density (trees/ha)	MAP (in) (range)	MAPS (in) (range)
Santiam Junction	44° 26' N 121° 57' W	1139	1979-2013	Douglas-fir	95.8	635.2	74.8 (54.8 – 108.4)	18.4 (2 – 38.4)
McKenzie	44° 13' N 121° 52' W	1454	1982-2013	mountain hemlock	50.4	417.9	98.2 (59.8 – 152.5)	44.4 (7.3 – 83.6)

ranges from 1 to 3‰, while intra-tree (circumferential) variability ranges from 0.5 to 1.5‰ (Leavitt, 2010). For our study, variations were minimized by sampling several cores per tree and pooling cellulose from eight trees. For isotope sampling, we extracted two to three 12-mm cores per tree from eight trees within each plot, at DBH (Phipps, 1985). In the vicinity of the plot, eleven additional trees were sampled with a 5.15 mm diameter increment corer to aid in cross-dating and ring-width analyses. Thus, we collected 27 cores at the Santiam Junction site and 33 cores at the McKenzie site for a total of 60 cores. Upon extraction from the tree, each core was sealed in a plastic tube for transport back to the laboratory for later analysis. The location of each sample site was documented using handheld GPS and each sampled tree was marked with flagging tape in case sites needed to be revisited (Table 1).

Core Processing for Ring-Width Measurement

Cores were attached to wooden mounts using standard wood glue with the long axis of the cells oriented vertically. Mounted cores were sanded with 180 grit paper and then 220 fine grit paper to remove scratches. This allowed easy visualization and differentiation between EW and LW bands in each annual ring. Cores were then dated and labeled according to age using a dot system (1 dot = 10 years, 2 dots = 50 years, 3 dots = 100 years). Manual cross-dating, matching ring width patterns between cores from the same tree and between trees visually to ensure each ring is assigned its correct year of formation, was completed before width measurement. Measurement of ring-width series was completed using a stereo microscope affixed over a Velmex ring-width encoder that measures to 0.001 mm precision. The microscope was interfaced with MeasureJ2X tree-ring measurement software on a desktop computer allowing management of ring-width series (VoorTech Consulting, http://www.voortech.com/projectj2x/). Cores were measured from earliest year of formation to the latest. The extent of measured years spanned from 1837 to 2013.

Measurement and cross-dating accuracy were quality checked using COFECHA software, with a segment size of 30 years and overlap of 15 years (Holmes, 1983; Grissino-Mayer, H.D., 2001). COFECHA creates a master sequence from all available series to correlate with segments of individual width series. Negative and low correlations show segments with potential errors or missing rings that need to be reexamined. Width series were split among sites and detrended using ARSTAN (Auto Regressive Standardization) software to produce ring-width chronologies (Cook, 1985). ARSTAN removes low-frequency components of ring-width variation due to endogenous age-related disturbances that are not produced by variations in climate. ARSTAN was run using batch mode processing with two curve fitting methods applied to the width series; a negative exponential and 100 year spline curve to remove low frequency variations (Cook and Kairiukstis, 1990).

Stable Carbon Isotope Analysis

The LW of each annual tree-ring was excised with a razor blade. Annual samples of LW were combined so each site had pooled yearly samples for the period of record. Pooling samples was instituted to reduce chemical preparation by 75%, while also reducing the time and costs of the study (Borella et al. 1998). Samples were then homogenized into a uniform fine powder using a Fisher Scientific™ PowerGen™ High-Throughput Homogenizer. Over 50 mg of ground sample was loaded into polyethylene-fiber filter bags (ANKOM, Fairport, NY), heat sealed and purified to holo-cellulose following the extraction methods of Leavitt and Danzer (1993). Hemi-cellulose was not extracted due to small sample size left over from pervious extractions. Year 2013 from the McKenzie site had no residual sample left. Subsequent analyses by continuous flow isotope ratio mass-spectrometry were performed at the CEOAS Stable Isotope Laboratory, Oregon State University to establish stable carbon isotope ($\delta^{13}C$) signals of ±.01 ‰ precision (Equation 1). Cellulose samples were weighed out to 1 ± .02 mg using an ultra-microbalance and loaded

into tin capsules which were combusted in an elemental analyzer (Carlo-Erba NA1500) coupled to a FinniganMAT delta Plus isotope ratio mass spectrometer. The resulting $\delta^{13}C$ signals were then converted to $\Delta^{13}C$ signals (Equation 2).

Description of Climate Data

We acquired measured snow data from the Natural Resources Conservation Service (NRCS) SNOpack TELemetry (SNOTEL) stations located at each of our collection sites (USDA, Natural Resource Conservation Service, http://www-.wcc.nrcs.usda.gov/snow). These stations are part of an extensive, automated system that measures snow water equivalent, which is a measure of the total amount of water represented by the snowpack. Temperature and total precipitation are also measured at SNOTEL sites. There are over 600 SNOTEL sites located in remote high-elevation watersheds of the western United States. SNOTEL sites use a pressure sensing snow pillow to measure SWE, a storage precipitation gage to measure snowfall plus rainfall, and an air temperature sensor. Historical measurements of mean daily and monthly SWE and precipitation for Santiam Junction and McKenzie were obtained from SNOTEL datasets. Peak SWE values were extracted from mean daily SWE datasets. Peak SWE, typically recorded near the end of March or on April 1st, acts as a primary measurement to characterize inter-annual variation in snowpack water content. Recording of daily and monthly SWE and precipitation extends back to 1979 for Santiam Junction and 1982 for McKenzie. Temperature data were more temporally limited and are also known to have significant quality control issues so we used data from the PRISM gridded climate data product (PRISM Climate Group Data & Products, http://www.prism.oregonstate.edu/explorer). Datasets acquired from PRISM included monthly minimum and maximum air temperatures (T_{min} and T_{max}, respectively) and dewpoint temperatures (T_{dew}). Average temperatures (T_{avg}) were calculated from the mean of T_{min} and T_{max}. Water vapor pressure deficit (VPD) and relative humidity RH were derived using

temperature data and the equations listed below, where P* is saturated vapor pressure and T (Eq. 4), represents either T_{max} when used in Eq. 5, T_{avg} when used for Eq. 6, or T_{dew}.

$$P^* = 617.4 + (42.22\ x\ T) + (1.675\ x\ T^2) + (0.01408\ x\ T^3) + (0.0005818\ x\ T^4) \qquad \text{(Eq. 4)}$$

$$VPD_{max} = \frac{P^*_{Tmax} - P^*_{Tdew}}{1000} = kPa \qquad \text{(Eq. 5)}$$

$$RH = \left(\frac{P^*_{Tdew}}{P^*_{Tavg}}\right)\ x\ 100 = \% \qquad \text{(Eq. 6)}$$

Growing season length was calculated conceptually, by means of a metric estimating approach, for each site using daily atmospheric temperature (T_{avg}) and SWE datasets. The number of days before July 15th since SWE was present and the number of days between January 1st and July 15th with temperatures above 5 ºC were counted for each year. Both of these counts should represent when the growing season begins for trees. However, even when SWE is zero, T_{min} may be too low for tree growth to ensue. Data were converted into standard scores (z-scores) as follows:

$$z = (X - \mu) / \sigma \qquad \text{(Eq. 7)}$$

where z is the z-score, X is the value of the element, μ is the population mean, and σ is the standard deviation. Z-scores represent the number of standard deviations a datum is from the mean. Conversion of both metrics to Z-scores allowed counts to be combined into a new Z-score simulating growing season length. After converting to Z-scores, the degree day values were deemed to be more important so they

were multiplied by a value of 0.7 while SWE z-scores were multiplied by a value of 0.3. These weighted Z-scores were then summed to create a value simulating growing season length.

Data Analysis

Pearson-product-moment correlation coefficients were calculated using Microsoft EXCEL to measure the linear correlation between climate variables and ring-width or $\Delta^{13}C$ data. SWE and other climate variables were used as the independent variable, while LW $\Delta^{13}C$ and detrended ring-width chronologies acted as the dependent variables.

Spatial Dimension

To provide a broader context for our study, a spatial dimension was added to the results presenting potential areas for future research that may experience similar trends between climate elements and tree-ring measurements as those we observed (Figure 2). A map of the western United States was created to show this spatial dimension using ArcGIS software (ESRI ArcGIS 10.2.2 for desktop, 2014). Map layers depicting the extent of tree species were based off the Atlas of United States Trees, Vol. 1 (Little, 1971). A raster of the seasonal snow zone in the western United States was acquired from the authors of Gleason et al. 2013. The seasonal snow zone is defined by pixels with 25% or more snow cover frequency. Snow cover frequency is defined as the ratio of the number of years when snow is observed comparative to the number of years in the period of record (Gleason et al., 2013) Additional map layers were all collected from the ArcGIS Online Database.

Results and Discussion

Environmental Data

Figure 3 shows mean monthly values of climate variables for both Santiam Junction and McKenzie. Trees growing at McKenzie potentially had considerably more access to water input from winter SWE. McKenzie had higher winter SWE and mean monthly SWE than Santiam junction during all months, especially after the date of peak SWE, around April 1st (Figure. 3A and Table. 2). Mean (and range) peak SWE was 18.4 (36.4), 44.4 (76.3) inches for Santiam Junction and McKenzie, respectively with more inter-annual variation (standard deviation) at McKenzie; 9.2, 15.6 inches. Both sites experienced lower precipitation during the months of July and August in the late summer when LW is primarily formed (Figure 3B and Table 2). Sites experienced relatively similar mean monthly and late summer relative humidity and maximum vapor pressure deficit with RH lowest and VPD_{max} highest during the late summer (Figure 3C, D and Table 2). In general, Santiam Junction had slightly higher mean monthly and late summer atmospheric temperatures, while also experiencing longer growing season length (Figure 3E, F and Table 2). Temperatures were highest during the growing season at both sites (Figure 3E).

Table 2. Climate data for Santiam Junction and McKenzie from SNOTEL and PRISM datasets. Abbreviations: WSWE, mean winter snow water equivalent; P_{LS}, mean late summer precipitation; RH_{LS}, mean late summer RH; VPD_{LS}, mean late summer maximum vapor pressure deficit; T_{LS}, mean late summer air temperature (T_{avg}); GSL, mean growing season length. Range is shown in parenthesis below mean values. Late summer (July to Sept.); winter (Dec. to March).

Site	SWE_W (in)	P_{LS} (in)	RH_{LS} (%)	VPD_{LS} (kPa)	T_{LS} (°C)	GSL (z-score)
Santiam Junction	39.2 (4.7 – 85.2)	4.2 (0.8 – 13.0)	55.0 (41.1 – 67.6)	1.7 (1.3 – 2.2)	14.4 (12.8 – 16.1)	31.9 (21.0 – 51.6)
McKenzie	91.6 (44.4 – 155.3)	5.6 (1.4 – 13.3)	55.8 (44.4 – 69.5)	1.9 (1.4 – 2.2)	13.1 (11.4 – 15.1)	22.4 (11.5 – 37.0)

Latewood $\Delta^{13}C$ and Width Data

Mountain hemlocks at the higher elevation site (McKenzie) had consistently less ^{13}C-enriched LW cellulose than Douglas-fir at Santiam Junction resulting in higher $\Delta^{13}C$ values (Figure 4). Mean (and range) of LW $\Delta^{13}C$ was 15.6 (2.3), 16.2 (1.7) ‰ for Douglas-fir and mountain hemlock, respectively. The maximum variation in LW $\Delta^{13}C$ between two consecutive years was 1.54, 1.06 ‰ for Douglas-fir and mountain hemlock, respectively. This suggests that LW $\Delta^{13}C$ represents inter-annual variation in moisture conditions at our selected sites. Douglas-fir experienced slightly more inter-annual variation (standard deviation) in LW $\Delta^{13}C$, 0.53 ‰, than mountain hemlock, 0.44 ‰. Correlation between $\Delta^{13}C$ chronologies at each site was $r = 0.74$, $p < 0.00001$ ($n = 31$), while correlation between detrended LW chronologies at each site was insignificant; $r = 0.20$, $p = 0.26$ ($n=32$). High correlation between $\Delta^{13}C$ chronologies of our sites and species suggests our trees responded coherently to the same moisture stress signals, whereas relation between inter-annual variations in LW width showed relatively little coherence and were unlikely to yield a strong climatic signal. Mean (and range) of detrended latewood width chronologies was 0.98 (0.50), 0.99 (0.73) for Douglas-fir and mountain hemlock, respectively (Figure 4). Mean between-tree variation (coefficient of variance) of detrended LW width chronologies was 0.28 for Douglas-fir and 0.37 for mountain hemlock.

Correlations between Tree-Ring Measurements and Environmental Data

Differences in correlation values between sites may be due to differences among site conditions or species physiology. Therefore, we focus primarily on the trends observed and not differences between sites or species. All significant correlations were either during the late summer, when LW primarily forms (late July to September), or the winter (Figure 5). Although highly significant trends did not carry over to both

sites, positive relationships between LW width and late summer RH, coinciding with negative correlations with late summer VPD_{max} and atmospheric temperature (T_{avg}) suggests that increasing evaporative demand, not only increases moisture stress, but also decreases growth (Table 3). Correlations with LW width did not corroborate observed trends shown in Figure 5 between LW $\Delta^{13}C$ and winter SWE or late summer precipitation. This suggests that although increased water supply influences moisture stress it may not be sufficiently important to growth at our selected sites or to our species to show any observable trends (Table 3). However, a number of correlations between LW width chronologies and climate variables were indefensible, biologically and did not follow expected trends displayed in previous studies which used similar methods (Roden & Ehleringer, 2007; Leavitt et al., 2010). As such we consider the few unexplainable relationships with ring-width variables to be spurious, a product of using a relatively short time series of approximately 35 and 32 years in length, reinforcing the need for a broader study between ring growth and SWE. Originally, a multiple linear regression model incorporating LW width analysis and stable isotope analysis was to be performed, but given the lack of fidelity among the LW width results at the two sites, we decided to focus primarily on Δ13C as a dependent variable.

Table 3. Pearson's correlation coefficients between climate variables and detrended latewood indices (LW) and the ratio of LW to total ring width indices (%LW). Abbreviations: WSWE, mean winter snow water equivalent; P_{LS}, mean late summer precipitation; RH_{LS}, mean late summer RH; VPD_{LS}, mean late summer maximum vapor pressure deficit; T_{LS}, mean late summer air temperature; GSL, mean growing season length. Significant correlations are indicated by asterisks: * $P < 0.05$, ** $P < 0.01$. Late summer (July to Sept.); winter (Dec. to March).

Site	Parameter	SWE_W	P_{LS}	RH_{LS}	VPD_{LS}	T_{LS}	GSL
Santiam Junction	LW	-0.06	0.04	0.53**	-0.22	-0.17	0.24
(n = 35 yrs.)	% LW	0.22	0.20	0.67**	-0.50**	-0.18	0.17
McKenzie	LW	0.32	0.10	0.11	-0.10	-0.15	0.02
(n = 32 yrs.)	% LW	0.28	0.32	-0.16	-0.18	-0.40*	-0.20

Figure 5 shows Pearson's correlation coefficients between climate elements and LW carbon isotope discrimination ($\Delta^{13}C$) for each site during the fall, winter, spring, and late summer. Late summer VPD_{max} and air temperature (T_{avg}) had highly significant negative correlations with LW $\Delta^{13}C$ implying that they were the primary drivers of $\Delta^{13}C$ and in theory moisture stress in our selected trees, $p < 0.01$ (Figure 5D, E). For years with higher temperatures (T_{avg}) and VPD_{max}, both sites experienced more evaporative demand, moisture stress, and lower $\Delta^{13}C$ values. A significant correlation between winter VPD_{max} and $\Delta^{13}C$ was observed in mountain hemlock ($p < 0.05$). This is probably a spurious relationship since VPD and air temperature are lowest during the winter months and should not affect tree growth or moisture stress (Figure 3E, D). T_{avg} and VPD_{max} were positively correlated at both sites for all recorded years ($p < 0.00001$, Figure 3E, D). Trends between air temperature (T_{avg}) and LW $\Delta^{13}C$ were similar to those of VPD_{max} (Figure 5D, E). Air temperature determines if precipitation falls as rain or snow during the winter months, influencing the relative contribution of winter precipitation that can subsidize the water budget at each site and thereby influencing LW $\Delta^{13}C$ during the late summer (Sproles et al., 2013). The relationship between air temperature and VPD may have accounted for the significant correlation observed between winter VPD_{max} and moisture stress in the late summer.

Growing season length showed a significant negative correlation with LW $\Delta^{13}C$ in mountain hemlock at the site with higher mean monthly SWE, implying that increased growing season length increases moisture stress, $p < 0.01$ (Figure 5F and Figure 3A). We speculate this is because with increased growing season length, snowpack melts earlier and trees have more time to expend available soil moisture so they experience increased moisture stress. Mountain hemlocks at the McKenzie site, which are adapted to snowy sub-alpine conditions, may be more sensitive to earlier snowmelt and a longer growing season length which agrees with the findings of Peterson & Peterson (2001). Mountain hemlocks located at lower elevation limits in the southern half of Oregon were predicted to experience increased summer drought

stress and reduced productivity as a result of earlier snowmelt and increasing temperatures from global climate change (Peterson & Peterson, 2001).

Climate elements which inhibited moisture stress all experienced positive trends with LW $\Delta^{13}C$ as was expected (Figure 5). Relative humidity during the late summer showed highly significant positive correlations with LW $\Delta^{13}C$ in both tree species, $p < 0.01$ (Figure 5C). Years with cooler air temperatures and lower VPD_{max} may have decreased transpiration from our selected trees during the growing period. Late summer precipitation had a significant positive correlation with LW $\Delta^{13}C$ at both sites implying that late summer rain events provided valuable moisture to our selected trees, $p < 0.01$ (Figure 5B). Winter SWE also showed a positive trend, supporting our hypothesis, with higher significance at McKenzie than Santiam Junction, $p < 0.01$; $p < 0.05$ (Figure 5A). Trends with $\Delta^{13}C$ for precipitation were the opposite of those with SWE patterns through the fall, spring, winter, and late summer. Collectively, these patterns suggest that in years where summer precipitation is low, trees in the Oregon Cascades will often rely on winter SWE as a moisture subsidy during the late growing season.

Figure 6 shows trends between peak SWE and LW $\Delta^{13}C$. Resulting trends between peak SWE and LW $\Delta^{13}C$ during the period of record were not statistically significant, $p > 0.05$ for both sites (Figure 6A, B). By combining z-scores of peak SWE from each site and comparing the ensuing value with a combined z-score of LW $\Delta^{13}C$ the resulting correlation verged on significance, $p > 0.05$ and undoubtedly would have reached significance with a longer period of record (Figure 5C). Thus, the sum of winter SWE provided a more reliable indicator of snowpack's contribution to our selected tree species than peak SWE. Figure 7 investigates this further by presenting correlations of mean monthly SWE vs. LW $\Delta^{13}C$ overlaid by lines which represent the accumulation and ablation of mean monthly SWE for each site. Mean December and January SWE had the most significant correlations with LW $\Delta^{13}C$ in the mountain hemlocks at McKenzie ($p < 0.01$). Douglas-fir at Santiam Junction showed significant correlations during December ($p < 0.05$).

June SWE also had a significant correlation with $\Delta^{13}C$ at McKenzie ($p < 0.05$), indicating that if delayed melt events occur, they may be used by mountain hemlocks in the late summer. Sites had the highest correlation values between SWE and LW $\Delta^{13}C$ in December and January despite SWE peaking each year during March or April. This trend was unexpected, but may potentially be due to large mid-winter melt events during December and January contributing to soil moisture content before springtime melt begins (Brooks et al., 2012). More research targeting a broader array of study sites and for a longer series of years must be completed to further understand this unexpected observation and the relative contribution of snowmelt to summer forest growth. Overall, our hypothesis was supported; the results from this study show that although winter SWE melts before tree growth starts, this water source often acts as a valuable late summer moisture subsidy to conifers in the McKenzie River Basin and montane forests of the Oregon Cascades.

Error Estimates and Limitations

There are multiple dimensions of error to consider for this study. Inter-tree and intra-tree variation in $\delta^{13}C$ were considered in the sampling strategy of tree core collection so it should have caused no large variations in $\Delta^{13}C$ series for each site. Potential error may have developed when choosing trees to be sampled; however, this error cannot be estimated and is negligible as many samples were collected from each site and pooled annually into homogeneous mixtures. Samples were also taken at locations not in the exact vicinity of the SNOTEL sites, but 0.25 km from the sites. Snow data may not be perfectly representative of the conditions of the sites from which trees were sampled. Selected tree-core collection sites were also chosen based on their vicinity to SNOTEL stations. In most traditional dendrochronology studies, sites are chosen which are hypothesized to increase the sensitivity of tree growth to a primary limiting climatic

factor. In this case we studied trees nearby to the SNOTEL sites, with little regard to factors that could constrain site water availability such as shallow soils overlaying basalt bedrock or thick volcanic scoria or coarse pumice and ash sediments, each of which could have increased the likelihood of finding trees with greater late-season moisture stress. Different tree species were also selected as a result of our sampling strategy and the location of our collection sites. Differences between species in phenology, leaf-level physiology, rooting-depth characteristics, or growth allocation may have caused minor variations in our results. However, we expect no large fluctuations in overall trends since tree species from the same genera and located in Oregon were observed to display similar growth rates and isotopic composition (Saffell et al, 2014). Potential errors may also have occurred during various phases of preparation and analyses. During the preparation of LW cellulose for isotopic analysis, excision of LW by razor blade may have been error prone and imperfect. Additionally, homogenization of powdered cellulose is never perfect. Thirdly, the time of year represented by LW may vary somewhat from year to year (affecting the dependent variable tree-ring $\Delta^{13}C$ or LW proportion), while the independent variables used (snowpack and meteorological data) have a more static timeframe. Intrinsic sample errors such as injuries or missing rings can pose as factors for error as well; however, cross-dating by COFECHA should have eliminated any errors during width measurement. This study was also limited to a short time frame of up to 35 years at the most, which may have largely impacted the LW width results, which were meant to support results from stable isotope analyses.

Conclusion

The overarching goal of this study was to distinguish the relationship between SWE and tree-ring $\Delta^{13}C$, to understand how snowpack may influence late summer moisture stress of coniferous mountain forests in the Oregon Cascades. We observed that in years with higher SWE, moisture stress was inhibited and there was an inverse relationship between subsequent winter snowpack and late summer moisture stress, supporting our hypothesis. Winter snowpack appears to have acted as a valuable moisture subsidy to the mountain forests in the Oregon Cascades we investigated. We expect that there is potential extent for this empirically-derived relationship to extend across similar elevations and in similar climatic conditions as the Oregon Cascades throughout the western United States (Figure 2), suggesting that there are a great many prospective locations for future research. Variations in ring width, density, structure, and the carbon, hydrogen, and oxygen isotopic composition of tree-rings and other organic matter can be used as proxies for a variety of climate parameters, including snowpack water content (McCarrol & Loader, 2004; Roden & Ehleringer, 2007; Leavitt et al., 2010). These types of tree-ring measurements, and $\Delta^{13}C$ in particular, should therefore be seen as a valuable resource for future studies evaluating how snow hydrology affects forest functioning.

This was the first quantitative study of how SWE might affect LW characteristics and $\Delta^{13}C$ in the McKenzie River Basin of the Oregon Cascades. Our results provide a valuable case study from the Oregon Cascades that can help inform future, widespread and in-depth investigations between snowpack and forest health. These investigations may be the most crucial in the Pacific Northwest, where snowpacks are projected to decline drastically by mid-century due to global climate change introducing drastic shifts in snowmelt, peak runoff, and determining whether precipitation falls as rain or snow (Sproles et al. 2013). By mid-century the sites we used in this study, and most sub-basin watersheds below 2000 m will no longer be capable of sustaining winter precipitation as snowpack (Sproles et al. 2013). For this reason it

is important for forest managers to consider the impending consequences of global climate change on snowpack within the Pacific Northwest, selecting more drought resistant tree species or adapting management practices to promote conservation of snowpack; snowpack which acts as a valuable source of moisture to the forests they manage.

Acknowledgements

Funding for this project was provided by the Bioresource Research (BRR) Department at Oregon State University (OSU). We thank K. Gleason for providing the seasonal snow zone raster file used in our spatial dimension map. We thank J. McKay at the College of Earth, Ocean, and Atmospheric Sciences (CEOAS) Stable Isotope Laboratory at OSU for her guidance when completing stable isotope analysis. We thank the USDA Forest Service Meinzer and Woodruff laboratories for the use of their instruments and laboratories. We thank K. Field, W. Crannell, L. Kayes, and the Mountain Hydroclimatology Research Group at OSU for their helpful feedback and advice throughout the course of this study. Lastly, we thank friends and family members who provided continued support.

References

1. Borella S., Leuenberger M., Saurer M. and Siegwolf R. (1998). Reducing uncertainties in δ13C analysis of tree rings: Pooling, milling, and cellulose extraction, Journal of Geophysical Research 103: doi: 10.1029/98JD01169. issn: 0148-0227.

2. Brooks J, Barnard H.R., Coulombe R, McDonnell J.J. (2010). Ecohydrologic separation of water between trees and streams in a Mediterranean climate, Nat Geosci 3, 100–104

3. Cook E. R. and Kairiukstis L. A. (1990). Methods of Dendrochronology: Applications in the Environmental Sciences. Springer. ISBN-13: 978-0-7923-0586-6.

4. Cook E.R. (1985). A Time Series Approach to Tree-Ring Standardization. Unpublished PhD Dissertation. University of Arizona, Tucson, AZ, USA

5. Craig H. (1957). Isotopic standards for carbon and oxygen and correction factors for mass spectrometric analysis of carbon dioxide, Goechimica et Cosmochimica Acta 12, 133–149.

6. Domec J.C. & Gartner B.L. (2002a). Age- and position-related changes in hydraulic versus mechanical dysfunction of xylem: inferrring the design criteria for Douglas-fir wood structure, Tree Physiology 22, 91–104.

7. Farquhar G.D., O'Leary M.H., Berry J.A. (1982). On the relationship between carbon isotope discrimination and the intercellular carbon dioxide concentration in leaves, Austral. J. Plant Physiol. 9, 121–137.

8. Gleason K. E., Nolin A.W., Roth T.R. (2013). Charred forests increase snowmelt: Effects of burned woody debris and incoming solar radiation on snow ablation, Geophysical Research Letters 40, 1–8.

9. Grissino-Mayer H.D. (2001). Evaluating cross-dating accuracy: a manual and tutorial for the computer program COFECHA, Tree-Ring Research 57, 205–221.

10. Holmes R.L. (1983). Computer assisted quality control in tree-ring dating and measurement, Tree-Ring Bulletin 43, 69–78.

11. Keeling C.D., Piper S.C., Bacastow R.B., Wahlen M, Whorf T.P., Heimann M, Meijer H.A. (2001). Exchanges of atmospheric CO_2 and $^{13}CO_2$ with the terrestrial biosphere and oceans from 1978 to 2000, I. Global aspects, SIO Reference Series, No. 01-06, Scripps Institution of Oceanography, San Diego, 88 pages.

12. Leavitt S.W. (2010). Tree-ring C-H-O isotope variability and sampling, Science of the Total Environment 408, 5244–5253.

13. Leavitt S.W., Danzer S.R. (1993). Method for batch processing small wood samples to holocellulose for stable-carbon isotope analysis, Anal. Chem. 65, 87–89.

14. Leavitt S.W., Woodhouse C.A., Castro C.L., Wright W.E., Meko D.M., Touchan R, Griffin D, Ciancarelli, B. (2011). The North American Monsoon in the U.S. Southwest: Potential for investigation with tree-ring carbon isotopes, Quaternary International, v. 235, p. 101–107.

15. Little E.L., Jr. (1971). Atlas of United States trees, volume 1, conifers and important hardwoods: U.S. Department of Agriculture Miscellaneous Publication 1146, 9 p., 200 maps.

16. Lux D.R. (1981). Geochronology. geochemistry. and petrogenesis of basaltic rocks from the western Cascades. Oregon: Columbus. Ohio. Ohio State University doctoral dissertation. 171 p.

17. McCarroll D., Loader N.J. (2004). Stable isotopes in tree rings, *Quat. Sci. Rev.* 23, 771–801.

18. Nelson D. B., Abbott M.B., Steinman B.A., Polissar P.J., Stansell N.D., Ortiz J.D., Rosenmeier M.F., Finney B.P., Riedel J (2011). A 6,000 year lake record of drought from the Pacific Northwest, Proc. Natl. Acad. Sci. U.S.A. 108, 3870–3875.

19. Peterson D.W., Peterson D.L. (2001). Mountain hemlock growth responds to climatic variability at annual and decadal time scales, Ecology 82, 3330–3345.

20. Phipps R. L. (1985). Collecting, Preparing, Crossdating, and Measuring Tree Increment Cores, US Geological Survey Water Resources Investigations Report 85-4148, 48 pp

21. Roden, J. S., Ehleringer J. R. (2007). Summer precipitation influences the stable oxygen and carbon isotopic composition of tree-ring cellulose in Pinus ponderosa, Tree Physiology 27, 491–501.

22. Saffell B.J., Meinzer F.C., Voelker S.L., Shaw D.C., Brooks J.R., Lachenbruch B, McKay J. (2014). Tree-ring stable isotopes record the impact of a foliar fungal pathogen on CO_2 assimilation and growth on Douglas-fir, Plant Cell Environ 37, 1536–1547.

23. Sproles E., Nolin A.W., Rittger K, Painter T (2013). Climate change impacts on maritime mountain snowpack in the Oregon Cascades, Hydrology and Earth System Science 17, 2581–2597.

24. Tague C, Grant G.E. (2004). A geological framework for interpreting the low flow regimes of Cascade streams, Willamette River Basin, Oregon, Water Resources Research, v40.

25. Trujillo E., Molotch N.P., Goulden M.L., Kelly A.E., Bales R.C. (2012). Elevation-dependent influence of snow accumulation on forest greening, Nature Geoscience 5, 705–709.

26. Van Mantgem P.J., Stephenson N.L., Byrne J.C., Daniels L.D., Franklin J.F., Fulé P.Z. et al. (2009). Widespread increase of tree mortality rates in the western United States, Science 323, 521–524.

27. Westerling A. L., Hidalgo H, Cayan D.R., Swetnam T (2006). Warming and Earlier Spring Increases Western US Forest Wildfire Activity, Science 313, 940–943.

28. Williams A.P., Allen C.D., Macalady A.K., Griffin D, Woodhouse C.A., Meko D.M., Swetnam T.W., Rauscher S.A., Seager R, Grissino-Mayer H.D. et al. (2013). Temperature as a potent driver of regional forest drought stress and tree mortality, Nature Climate Change 3, 292–297.

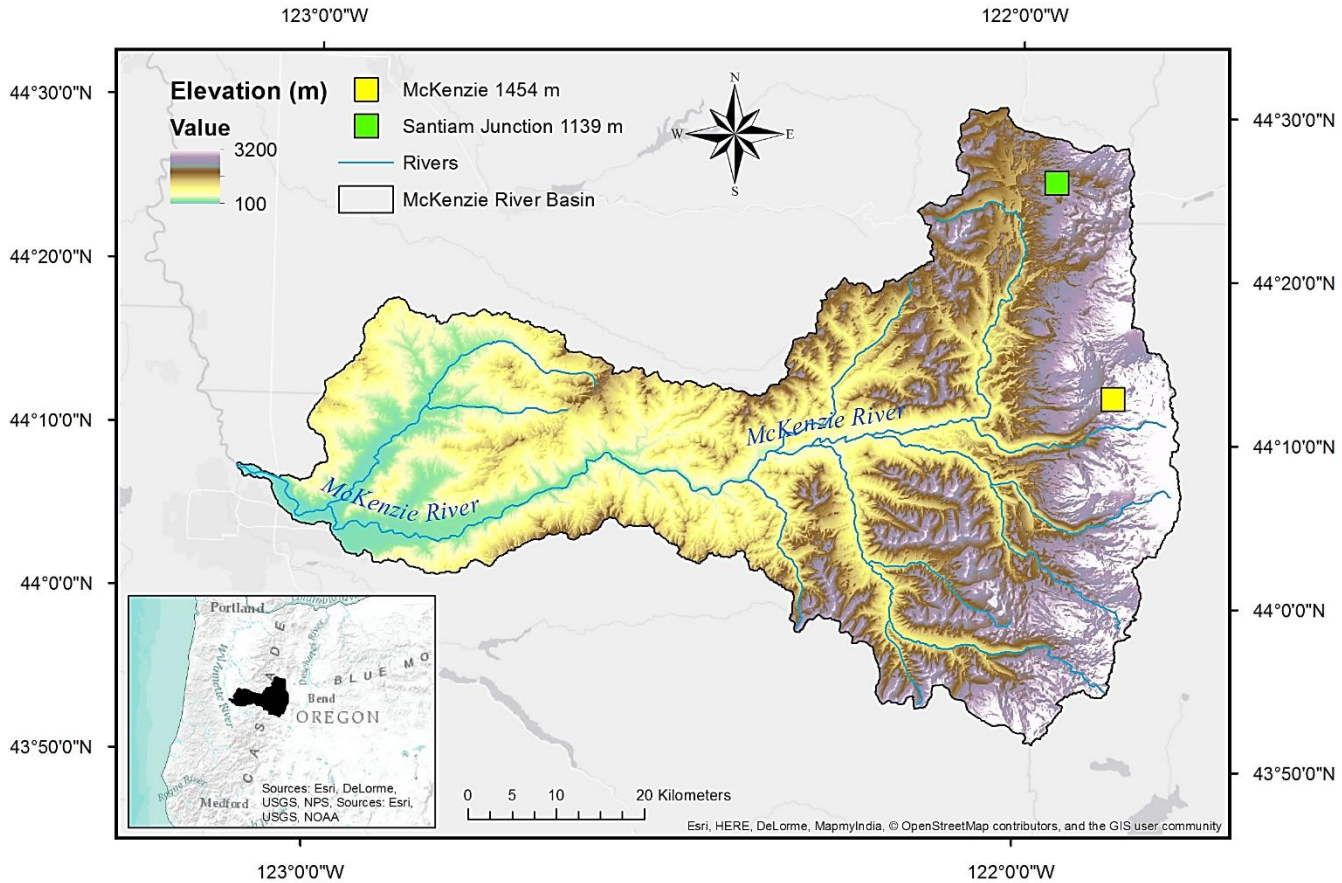

Figure. 1 Context map of the study area created in ArcGIS displaying the McKenzie River Basin Watershed and our collection sites in the Oregon Cascades.

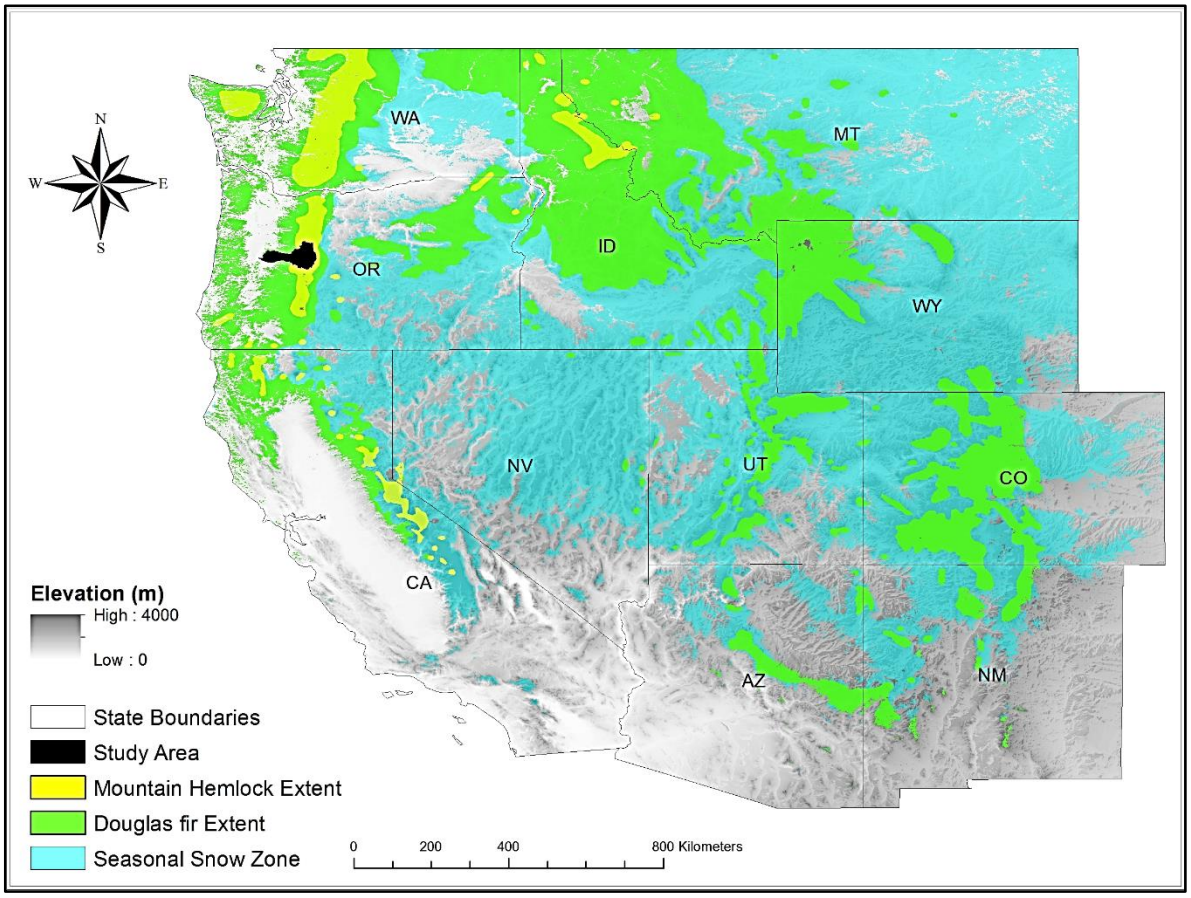

Figure. 2 Map of the spatial extent of our study created in ArcGIS displaying the study area and the extent of both tree species within the seasonal snow zone.

.

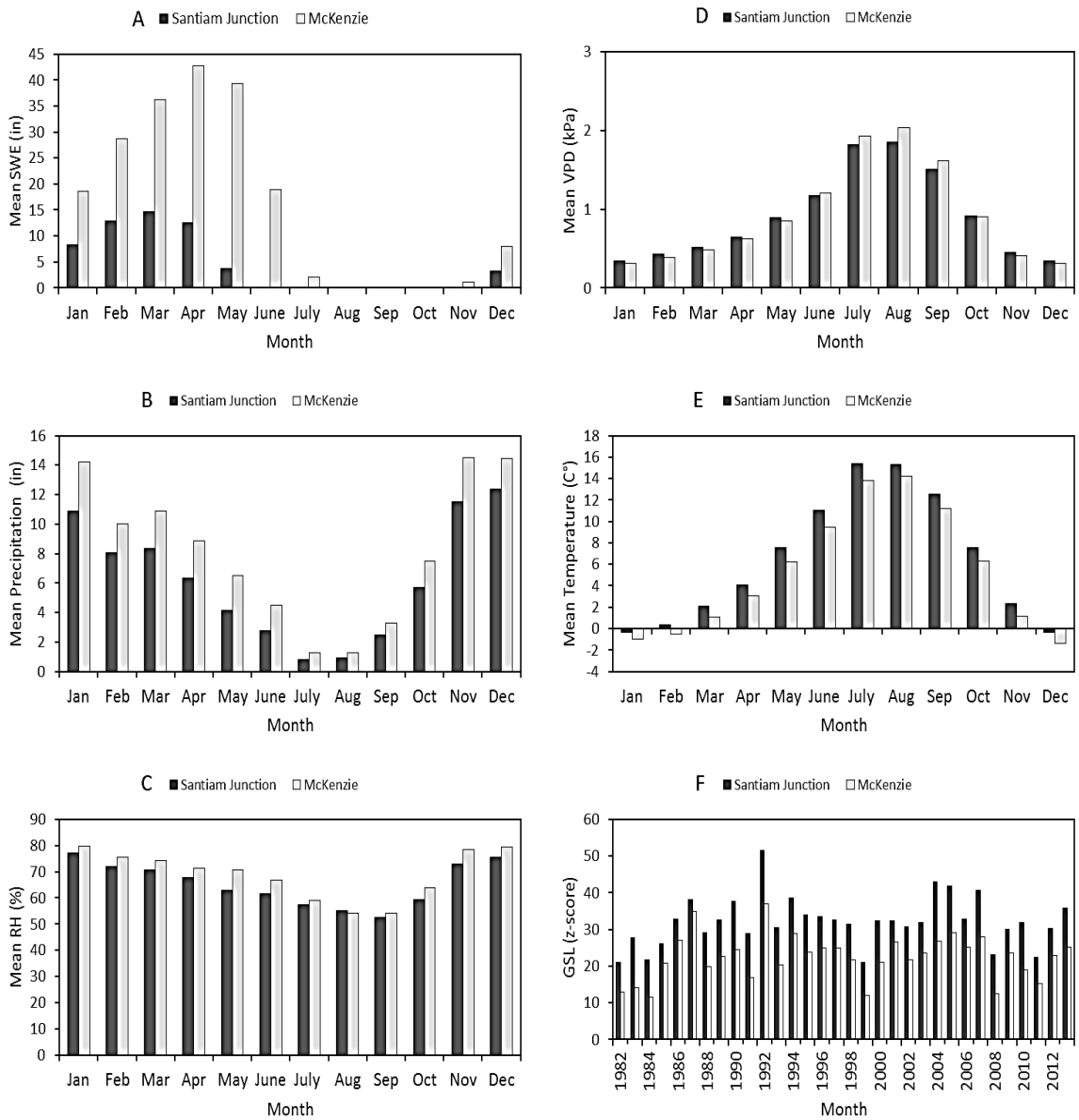

Figure 3. Mean monthly snow water equivalent, precipitation, relative humidity, maximum vapor pressure deficit, and air temperature (T_{avg}) from SNOTEL and PRISM datasets for McKenzie and Santiam Junction (Panel A – E). Panel F shows annual growing season length for each site.

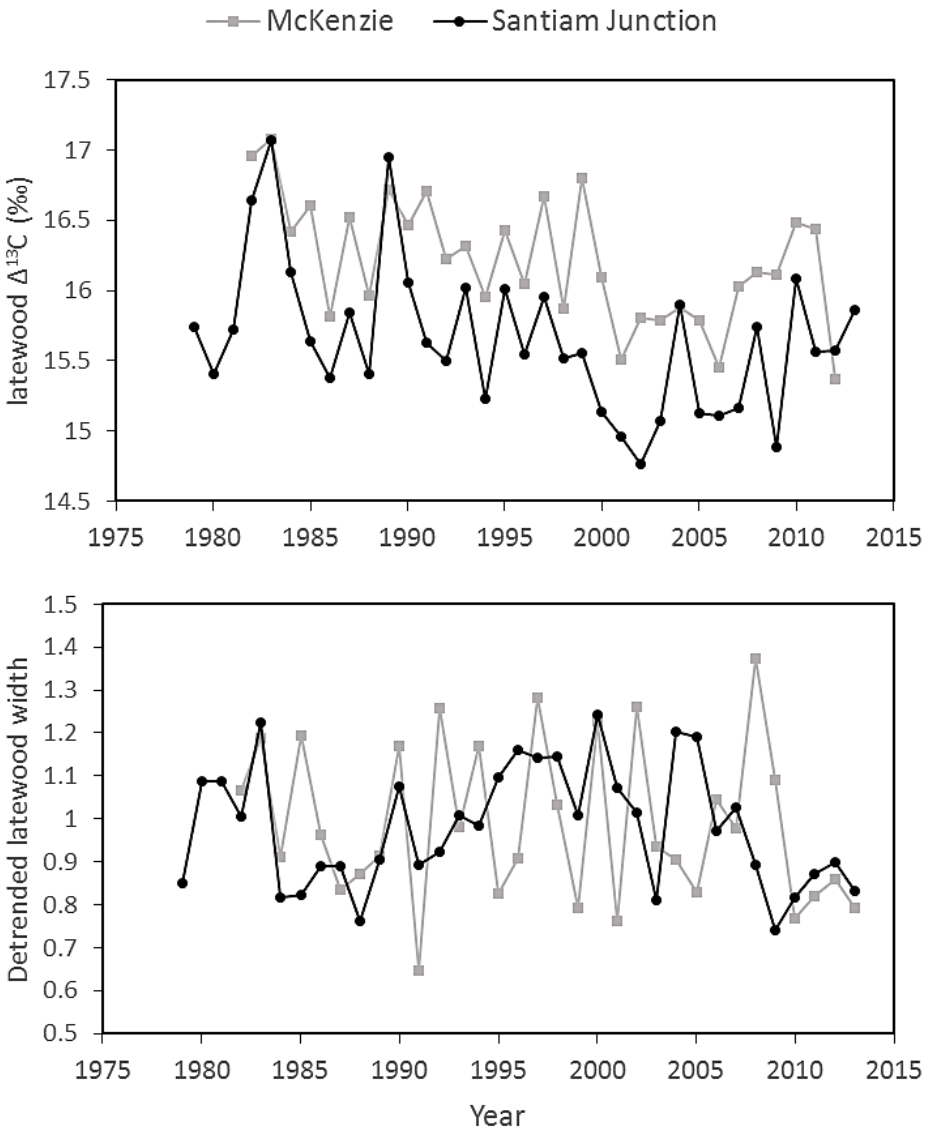

Figure 4. Time series of latewood carbon isotope discrimination ($\Delta^{13}C$) and mean detrended LW width chronologies for Douglas-fir (Santiam Junction) and mountain hemlock (McKenzie).

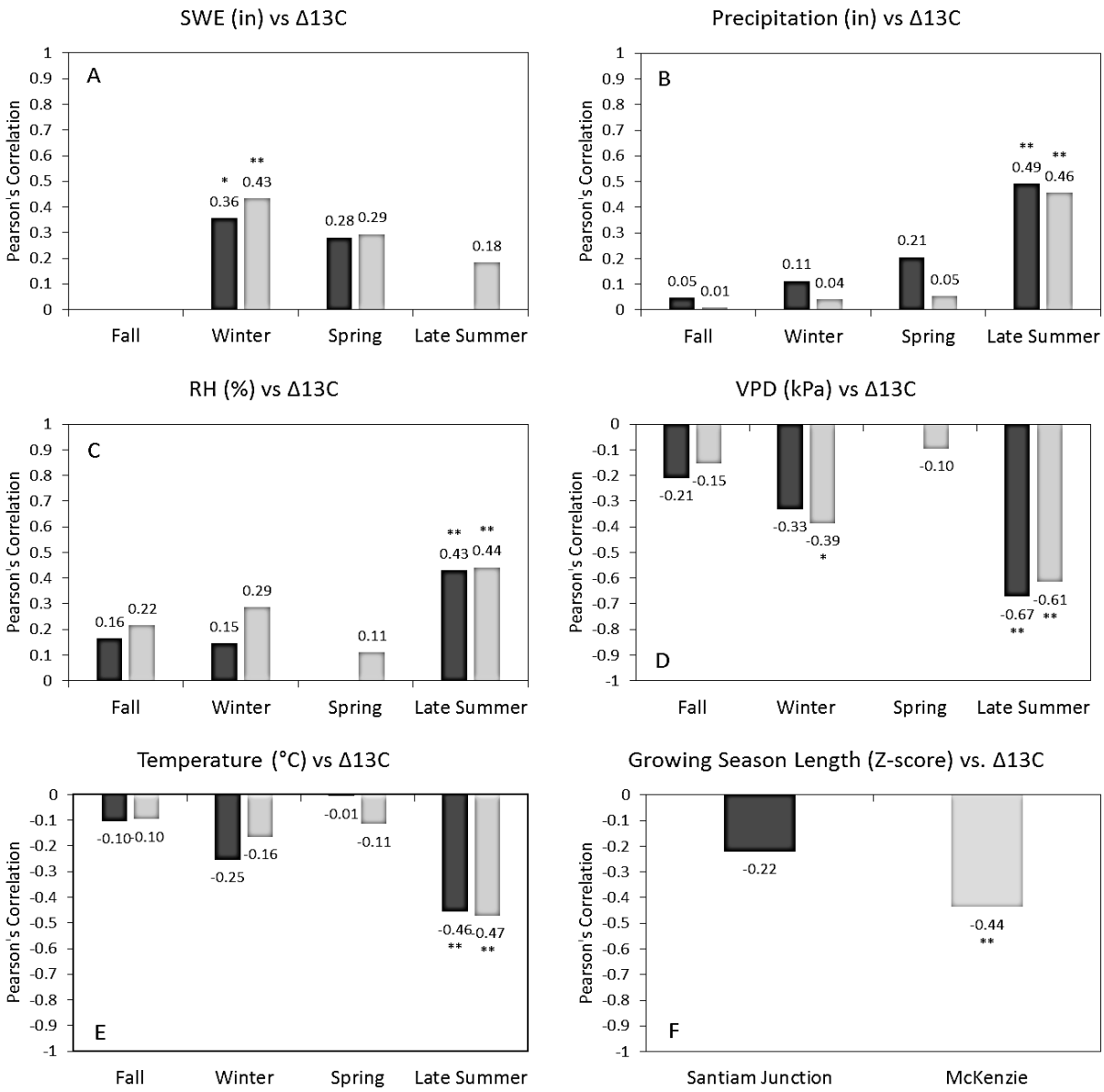

Figure 5. Correlations between climate variables and annual carbon isotope discrimination ($\Delta^{13}C$) in latewood for Santiam Junction (dark grey, n = 35 yrs.) and McKenzie (light grey, n = 31 yrs.). SWE and precipitation are from SNOTEL datasets, while the rest of the climate datasets are PRISM modeled. Pearson's Correlation Coefficient (y-axis) depicts the correlation between variables by season and between sites (x-axis). Seasons: Fall (Aug. to Oct.), winter (Dec. to March), spring (March to May), late summer (July to Sept.). Significant correlations are indicated by asterisks: * $P < 0.05$, ** $P < 0.01$.

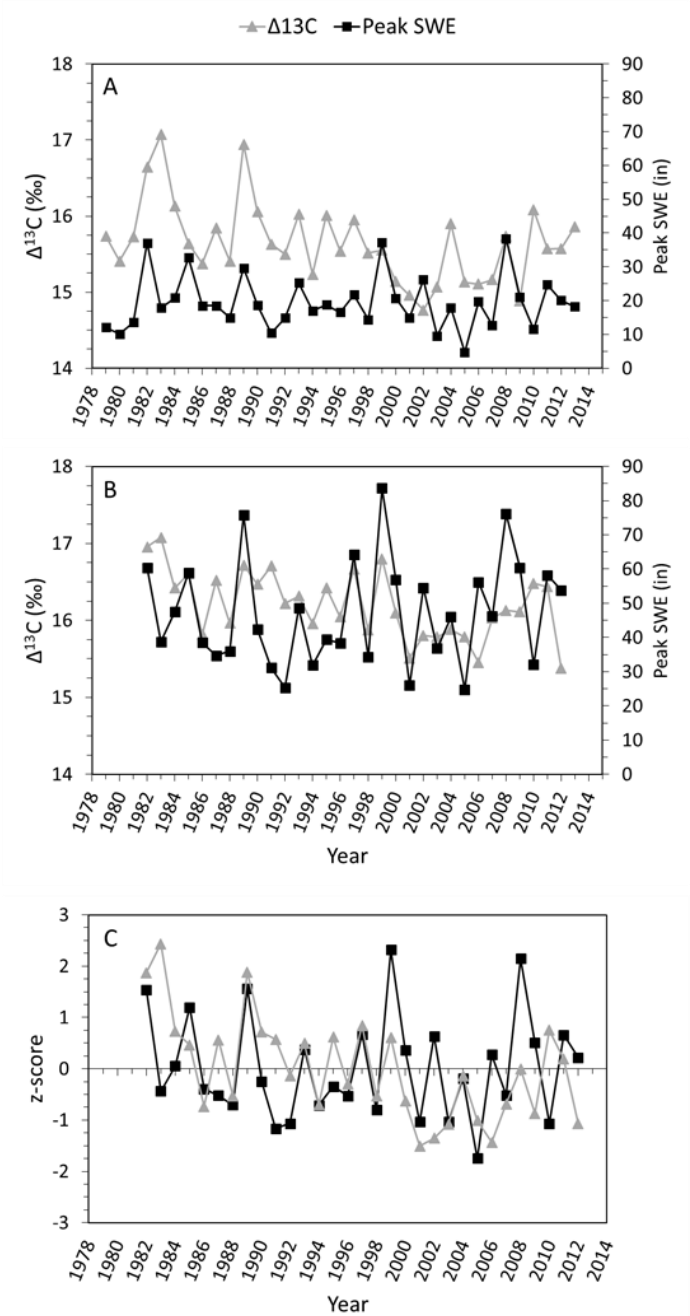

Figure 6. Time series of LW $\Delta^{13}C$ versus peak SWE for each site (Panel A, B) and the combined z-score of LW $\Delta^{13}C$ versus the combined z-score of peak SWE (Panel C).

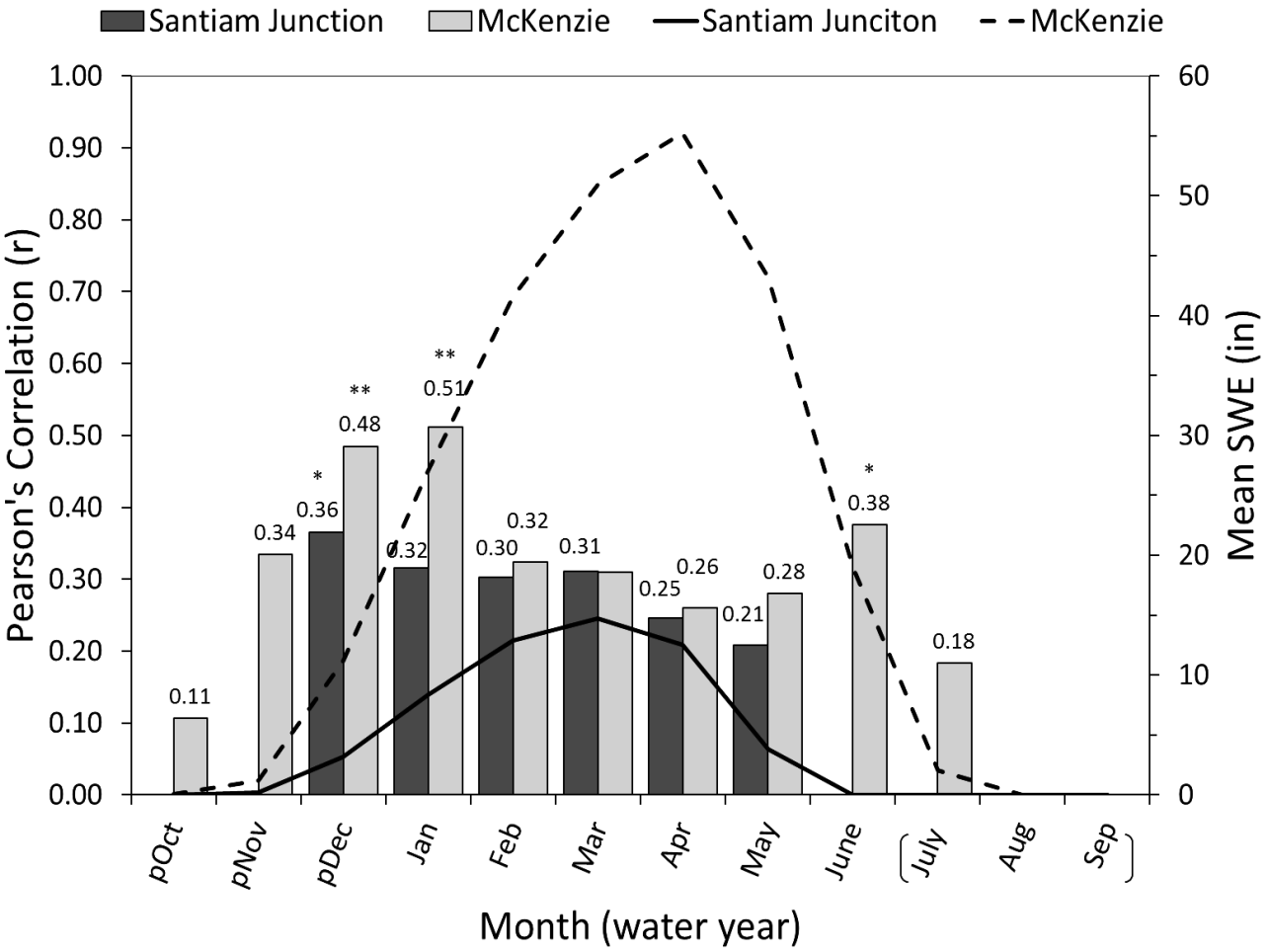

Figure 7. Pearson correlation coefficient values (bars) of mean monthly SWE vs. latewood $\Delta^{13}C$ for Santiam Junction (n = 35 yrs.) and McKenzie (n = 31 yrs.). Mean monthly SWE for each site is represented by stacked lines. Brackets are around the late growing season when latewood forms. Significant correlations are indicated by asterisks: * $P < 0.05$, ** $P < 0.01$.